

BIBECHANA

ISSN 2091-0762 (Print), 2382-5340 (Online)

Journal homepage: <http://nepjol.info/index.php/BIBECHANA>

Publisher: Department of Physics, Mahendra Morang A.M. Campus, TU, Biratnagar, Nepal

GPS TEC Scintillations and TEC depletion as seen from Hetauda and NAST, Nepal for 2016

Basu Dev Ghimire^{1, 2, 3, 5, *}, Narayan Prasad Chapagain⁴, Balaram Khadka^{2, 3}, Gambir Bidari², Karan Bhatta^{3, 5}, Aditay Singh Thapa²

¹Institute of Science and Technology, Central Department of Physics , Tribhuvan University

²St. Xavier's College , Maitighar Kathmandu , Nepa

³Nepalese Center for Research in Physical Sciences (NCRPS)

⁴Amrit Campus , Tribhuvan University, Kathmandu Nepal

⁵Gyan Research Academy for Communication and Education (GRACE), Kathmandu Nepal

*Email: basu.ghimire99@gmail.com

Article Information:

Received: December 25, 2020

Accepted: May 13, 2021

Keywords:

GPS TEC

ROTI

S₄ index

PRN

ROTI and S₄ correlation

ABSTRACT

We analyzed Global positioning System Total Electron Content (GPS-TEC) data of stations Hetauda (27.414 °N and 85.051 °E) and NAST (27.656 °N and 85.327 °E), Nepal which are a part of UNAVCO. We obtained the variation of rate of TEC index (ROTI) and S₄ index throughout the year 2016 for the two stations involved for the 32 all the Pseudo Random Noise (PRN) numbers barring PRN number 4 which was inactive throughout the year. We chooses two stations data which are almost 40 km in distance and correlated the value of ROTI index with ROTI index and S₄ index with S₄ index and found that the ROTI index of Hetauda is well correlated with ROTI index of NAST with the highest being 94% for PRN 10 and the lowest being -13% for PRN 1. Extremely low correlation between S₄ index of Hetauda and S₄ index of NAST was observed with the highest correlation being 8% in PRN 3, 32 and the lowest correlation of -15% in PRN 12.

DOI: <https://doi.org/10.3126/bibechana.v18i2.33405>

This work is licensed under the Creative Commons CC BY-NC License. <https://creativecommons.org/licenses/by-nc/4.0/>

1. Introduction

The ionosphere is composed of charged particles: ions and electrons. The composition of ionosphere varies with change of seasons, solar cycle, solar intensity and geomagnetic storms [1]. One of the major factors that causes variation in composition of ionosphere is sunlight, which ionizes gas molecules with its ultraviolet rays and releases free

electrons. As the number of free electrons varies in ionosphere, so does the electron density in the ionosphere. It is one of the significant reasons for observation of major difference in electron density of day and night. This electron density is commonly defined as total electron content (TEC)

$$TEC = \int_{Receiver}^{Satellite} N. ds$$

where, N is electron density.

TEC is dependent on its path. This expression gives Slant TEC (STEC) when the electron density along the ray path of the satellite to receiver is taken into account. While the Vertical TEC (VTEC) can be obtained, when the electron density along the perpendicular path of the satellite to receiver is taken into account [2].

Global Position System (GPS) can be used to measure the change in the electron and ion content of ionosphere, as the GPS signal's characteristics changes while passing through the ionosphere. As GPS signal travels through the ionosphere, it attenuates, delays, it's level of attenuation, delays are determined by time it travels through the ionosphere. The ionosphere is dispersive, which means that the apparent time delay contributed by the ionosphere depends on the frequency of the signal [3, 4].

The STEC is obtained from the dual frequency code measurements using the relation [2] as in equation (1).

$$STEC = \frac{1}{40.3} \times \left(\frac{1}{L_1^2} - \frac{1}{L_2^2} \right)^{-1} \times (P1 - P2) + TEC_{CAL} \quad (1)$$

where P1 is the Pseudo range at L1 (it is at 1575.42 MHz (10.23 MHz × 154)); P2 is the Pseudo range at L2 (it is at 1227.60 MHz (10.23 MHz × 120)), TEC_{CAL} is the bias error correction. STEC measured by the receiver at every 30s is used. The measured STEC is corrected for the receiver differential delay TEC_{CAL} .

In the above equation (1), TEC_{CAL} represents the bias error correction and is different for different satellite-receiver pairs [2] which is calculated from CODE error. Slant TEC is dependent on the ray path geometry through the ionosphere and an equivalent vertical value of TEC, which is independent of the elevation of the ray path, is calculated [5].

There are two universally accepted quantities, the amplitude/phase scintillation $S_4/\partial\phi$ and ROTI that are commonly used to quantitatively describe ionospheric variations which are usually TEC

fluctuations. The amplitude scintillation index, S_4 , is the normalized root-mean square (RMS) deviation of irradiance, I [6]. Measurements of both S_4 and $\partial\phi$ can be derived from Global Navigation Satellite System (GNSS) scintillation monitoring receivers sampled at high frequencies, but the number and regional/global distribution of scintillation monitoring receivers are limited due to high costs. This scarcity of scintillation monitoring receivers restricts the extensive use of $S_4/\partial\phi$ indices [7-12]. The TEC fluctuation index ROTI (which is derived from ordinary non-scintillation GNSS receivers sampled at low frequencies) was first proposed by Pi et al [7, 10, 12] in 1997. After that, ROTI has been used universally to quantitatively describe ionospheric anomalies. ROTI is the standard deviation of the rate of TEC (ROT) in a given 5 min interval. Many studies have shown a close correlation between S_4 and ROTI [10, 12-15].

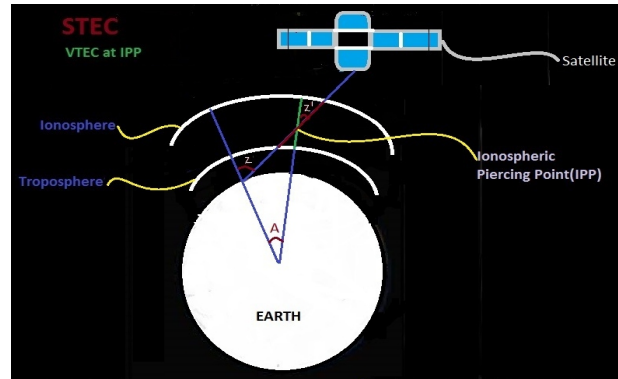


Fig. 1: Vertical Total Electron Content (VTEC).

TEC, S_4 data are taken by many satellites at a time. Hence, the data are different from each other due to their different activation time. In order to increase the reliability of these data, the data should be separated according to their satellites. These different satellites can be separated by their Pseudorandom noise (PRN). The PRN codes help in identification of the satellite by a receiver, while it is receiving its data. PRN are used as an identification measure in code division multiple access (CDMA) based satellite navigation system

[16]. Satellite throughout the world within a GNSS constellation has a unique PRN code that it transmits as part of the Civilian Access navigation message, which allows receiver to identify exactly which satellite(s) it is receiving [17].

2. Materials and Methods

The rate of TEC (ROT, in TECU/min) and amplitude scintillation index S_4 is measured by utilizing dual-frequency GPS observation phase data [7]. Rate of TEC abbreviated as ROT computes the relative TEC changes, along the signal paths from each individual to the receiver, as shown in equation (2) [12]. ROTI Index is the standard deviation of ROT over a 5 min interval in TECU/min in equation (3) [7].

$$ROT = (\Delta STEC) / \Delta t \quad (2)$$

$$ROTI = \sqrt{\langle ROT^2 \rangle - \langle ROT \rangle^2} \quad (3)$$

where STEC is the TEC along the ray path from the satellite to the receiver (in TECU/min) and Δt in minutes represents the sampling interval.

The amplitude scintillation index, S_4 , is the normalized root-mean square (RMS) deviation of irradiance, I [6] as in equation (4).

$$S_4 = \sqrt{\frac{\langle I^2 \rangle - \langle I \rangle^2}{\langle I \rangle^2}} \quad (4)$$

Data Availability

In this study, dual-frequency GPS data was made public by UNAVCO

(<https://www.unavco.org/data/gps-gnss/data-access-methods/dai2/app/dai2.html#4Char=NAST;scope=Station;sampleRate=normal;4CharMod=startsWith.>)

UNAVCO has provided civilian access to the dual-frequency GPS data of its different receiver stations. The data is available in 1.0 Compact RINEX version files. We processed the data using GPS TEC analysis software developed by Gopi Seemala, affiliated to the Indian Institute of Geomagnetism. The software converts the RINEX data into ASCII format separating data into various columns where values of STEC, VTEC, S_4 index

are separated according to PRN numbers. We processed those ASCII files and found yearly variation of ROTI and S_4 for all the PRN numbers. For studying correlation of ROTI and S_4 , we calculated a single value of ROTI for one day (by taking the average), did the same for S_4 index and found out individual values of ROTI and S_4 for each day of 2016 for the two stations involved and found the correlation between S_4 and ROTI.

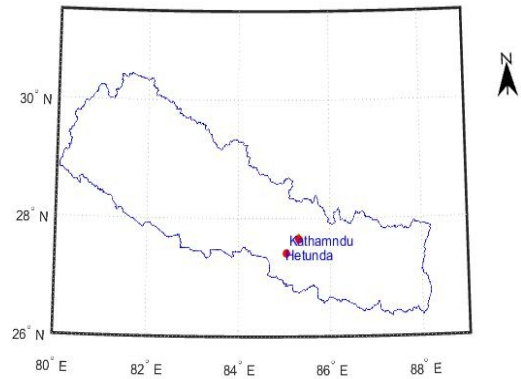


Fig. 2: Map of Nepal showing two GPS stations taken in our study.

3. Results and Discussions

Variation of ROTI

Figure 3 and 4 give us a pictorial description of the change in ROTI index from two stations of Nepal; Hetauda and NAST, respectively during 2016. Besides, PRN 4 was inactive during 2016. Technically, Figure 1 gives the variation of ROTI + 200xPRN with days. The reason for addition of 200 as a factor to the PRN number is that the maximum value of ROTI did not exceed 200 for Hetauda. We changed the factor 200 (multiplied to PRN) to 400 in NAST as the maximum value of ROTI in 2016 ranged in the high as three hundred. The lowest horizontal line in Figures 3 and 4 represents the ROTI for PRN 1, succeeded by PRN 2 and so forth such that the highest vertical line represents the variation of ROTI for PRN 32.

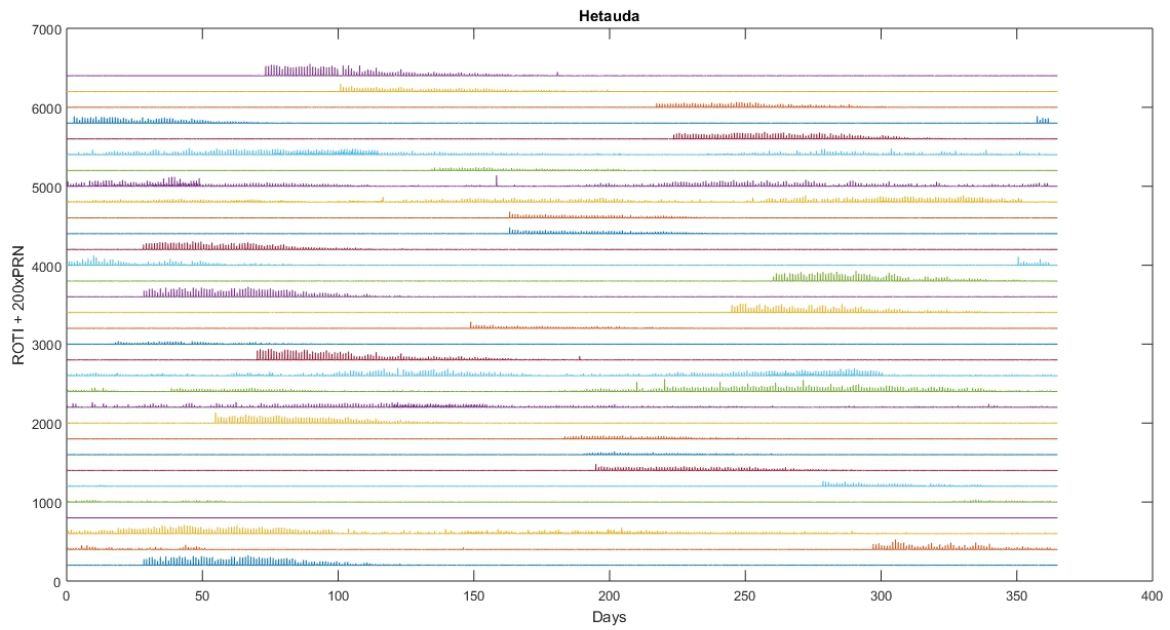


Fig. 3: Variation of ROTI index during 2016 in Hetauda, in units of TECU/min.

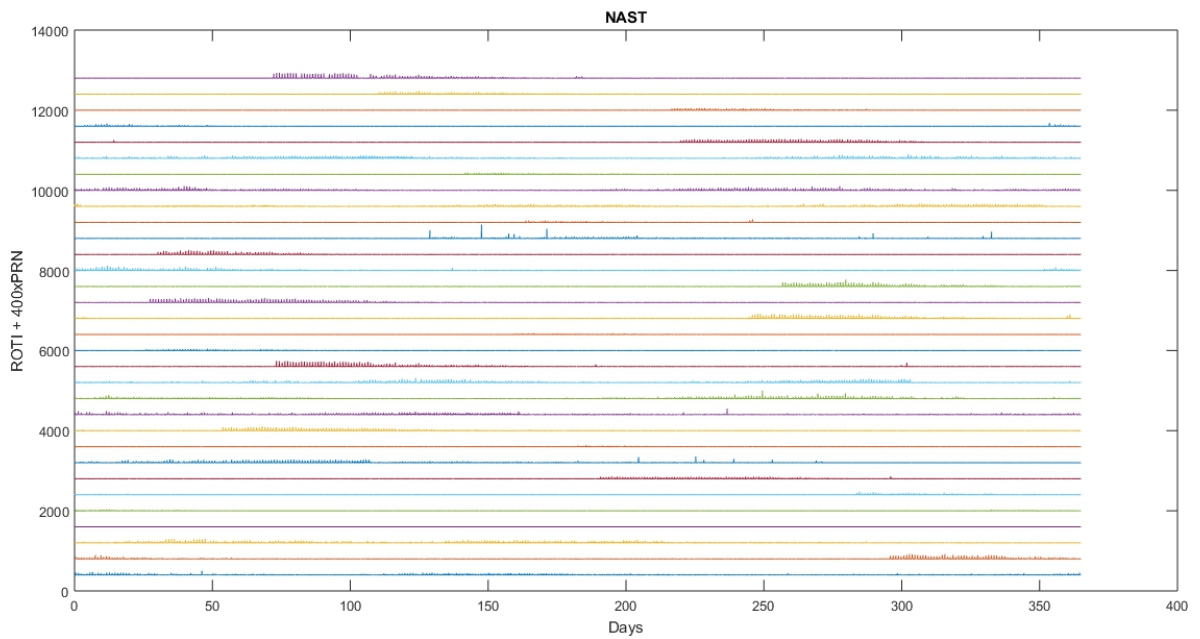


Fig. 4: Variation of ROTI index during 2016 in NAST, in units of TECU/min.

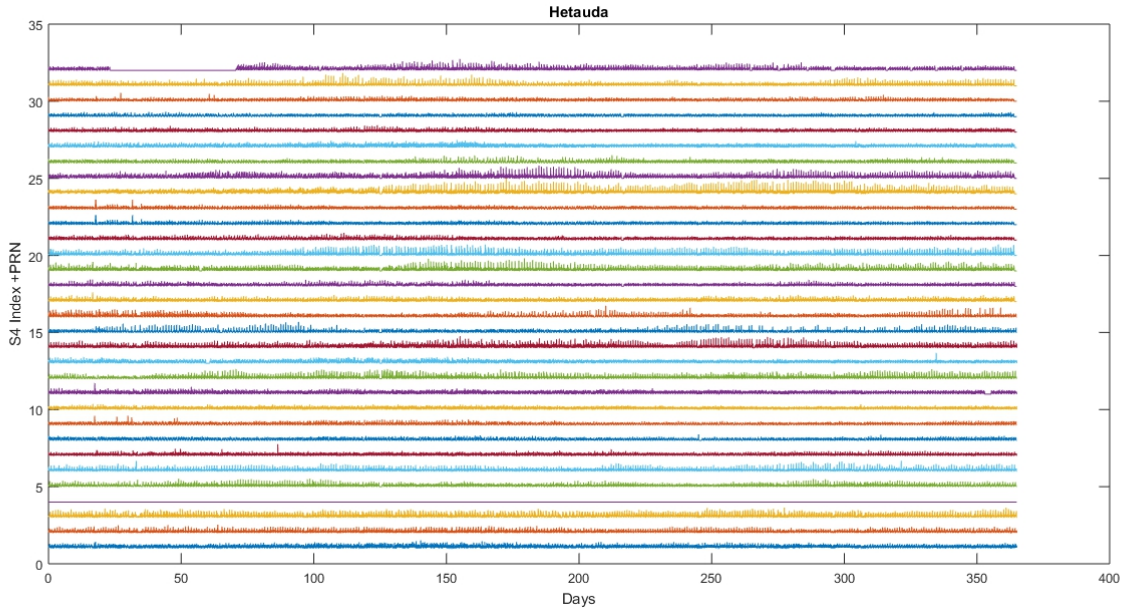


Fig. 5: Variation of S4 index in Hetauda during 2016.

In Hetauda, we observed that the values of ROTI were high only for a specific time of the year. PRN 1, 18 and 21 show high values of ROTI in around exactly the same time of the year during February and March. The same can be said about PRN 14 and 32 which show high values of ROTI from mid-March until April. The fourth horizontal line from the bottom is static because we had no data of STEC for PRN 4.

Similar patterns of extended period of months where the values of ROTI index were high. However, for PRN 9, 12 and 22, we can see that elevated values of ROTI can be seen, not for extended periods of months but only for single days.

Variation of S4 index

The lowest horizontal line in Figures 5 and 6 represents the S4 for PRN 1, succeeded by PRN 2 and so forth such that the highest vertical line represents the variation of ROTI for PRN 32. In both stations, Hetauda and NAST, the beginning of February to the middle of March, no values of S4 index was recorded by PRN 32. As PRN 4 was inactive, we have a flat line for the S4 index for PRN 4. For PRN 25, we observed consistently high values for PRN 25 during July in Hetauda. Very

high values of S4 index for PRN 24 was observed in the months of September and October. The same was true of PRN 14 as well. Although the values of S4 was consistently low throughout the year for PRN 7, 9, 11, 22 and 23, there were a few days where the values of S4 index were high enough.

In NAST consistently high values of S4 index were observed for almost all PRN except PRN 6, 13, 27 where the values of S4 was mild throughout the year.

Correlation between ROTI from two stations

Figure 7 and 8 show dynamic correlation between ROTI of Hetauda and of NAST, along with S4 index of Hetauda and of NAST in 2016. We did observe a good correlation between the ROTI of two different stations but did not observe any good correlation between S4 index of Hetauda and NAST. However, the results show a negative correlation between ROTI of Hetauda and ROTI of NAST. For S4 index, 17 PRNs revealed negative correlation between Hetauda and NAST, while just PRN 1 pointed to negative correlation between ROTI of Hetauda and NAST.

For ROTI, 1 PRN showed a positive correlation of less than 10% while for S4 index 8 out of the 14 PRNs that had a positive correlation had a correlation of less than 10% and PRN 7, 21, 30 had a correlation of 0.

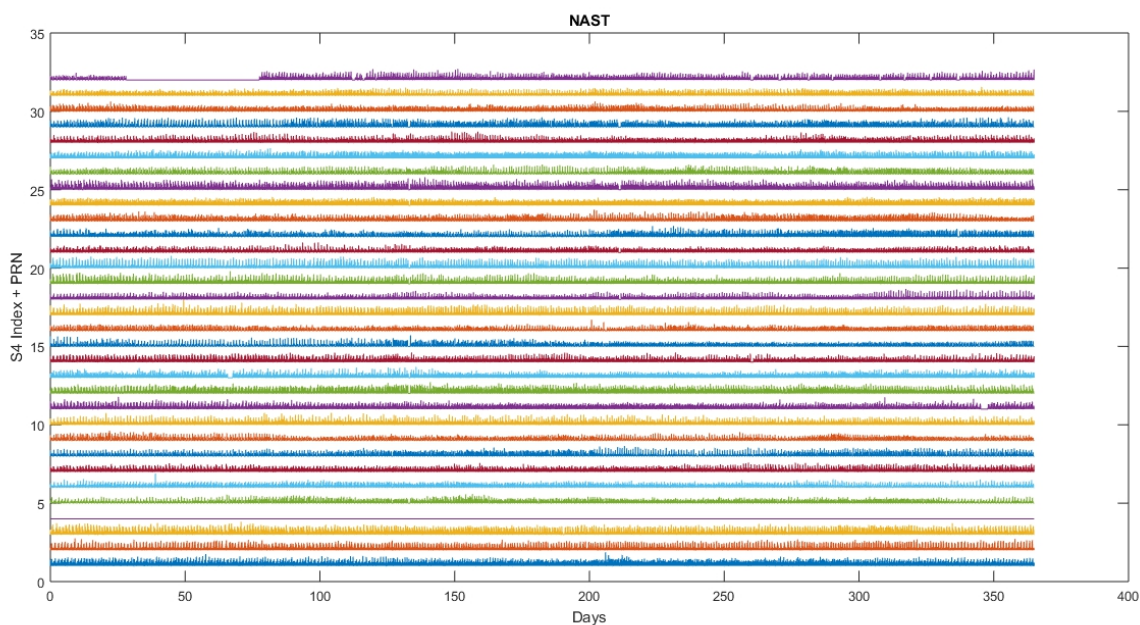


Fig. 6: Variation of S4 index in Nast during 2016.

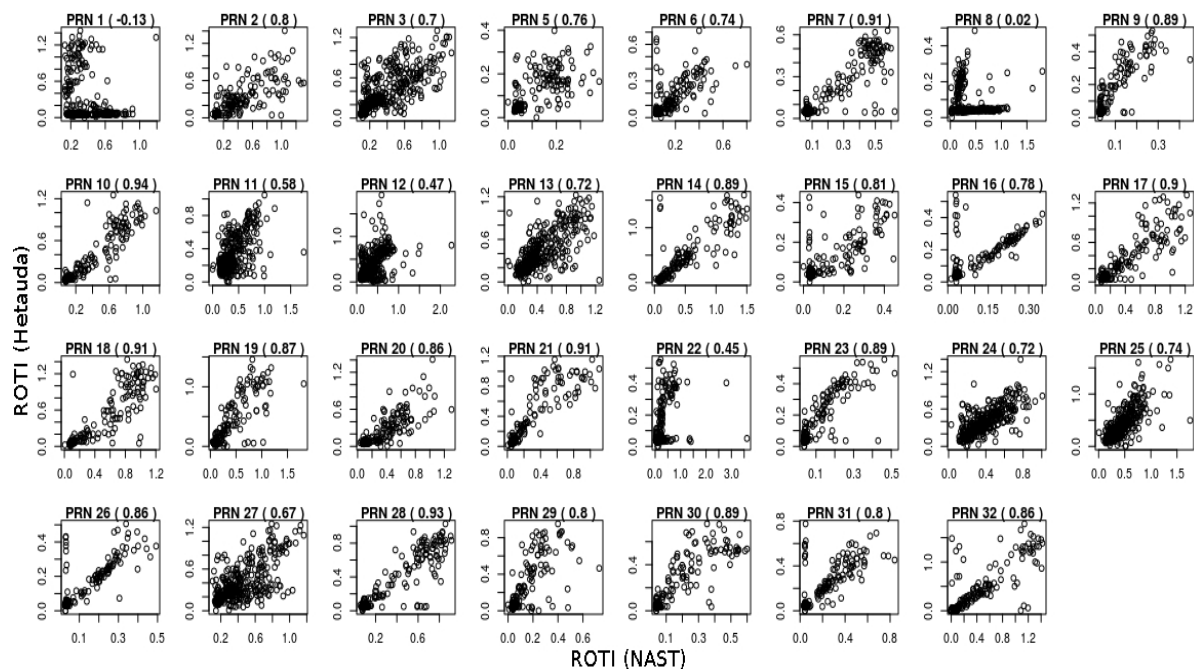


Fig. 7: Correlation between ROTI from two stations at Hetauda and NAST.

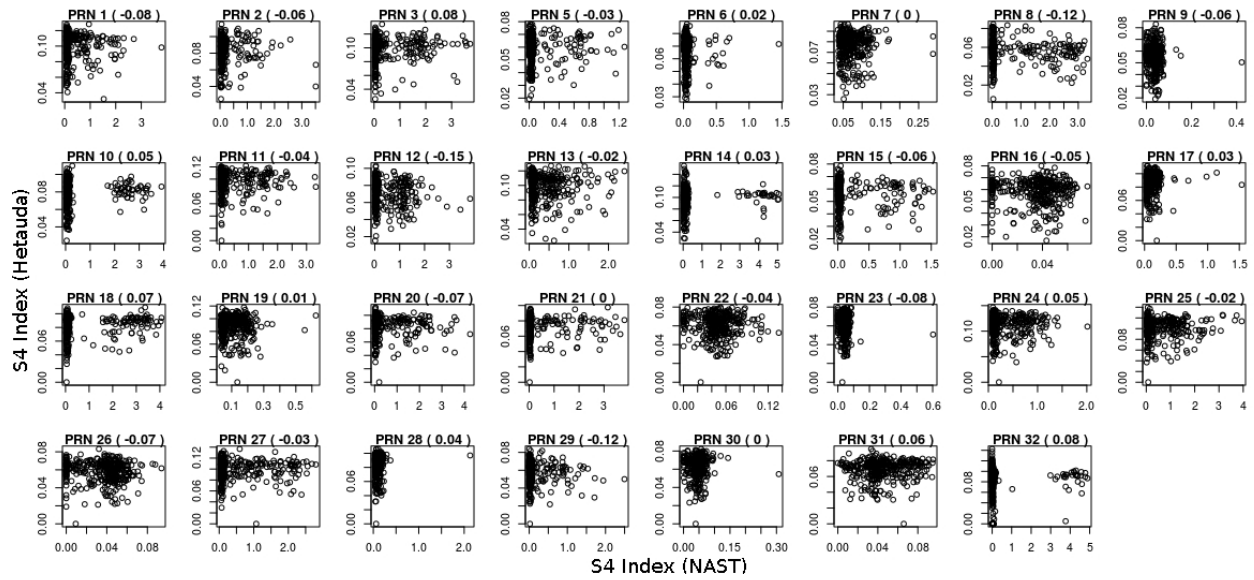


Fig. 8: Correlation between S4 index from two stations at Hetauda and NAST.

4. Conclusion

The values of ROTI and S₄ index were abruptly high in a few days when the values in other days in closer proximity were relatively small might have been due to the variation in geomagnetic parameters or might have its origins in Equatorial Ionization Anomaly (EIA), which greatly affects the values of TEC in regions close to the equator. Furthermore, the high correlation between ROTI of Hetauda and NAST, whereas low correlation between S₄ of Hetauda and NAST might suggest that there is a correlation between the ROTI of different stations but no correlation between S₄ in Nepal. However, before concluding this result, we have to carry out the detail analysis of the correlation between the two parameters, ROTI, and S₄ index throughout Nepal.

It is possible that due to geomagnetic storms and EIA, good correlation was not observed in the two stations where we conducted our study. Therefore, a detailed analysis of the ROTI, and S₄ index throughout Nepal will give a clearer picture of the TEC variation in Nepal.

Acknowledgement

We would like to thank University grant commission Nepal, provide fund for this research work. We would also like to thank UNAVCO and Gopi Seemala for providing the data and TEC software

References

- [1] R. Tiwari, S. Bhattacharya, P. Purohit and A. Gwal, Effect of TEC variation on GPS precise point at low latitude, The Open Atmospheric Science Journal 3 (2009) 3. <https://doi.org/10.2174/1874282300903010001>
- [2] M. S. Bagiya, H. Joshi, K. N. Iyer, M. Aggarwal, S. Ravindran, S & B. M. Pathan, TEC variations during low solar activity period (2005–2007) near the Equatorial Ionospheric Anomaly Crest region in India, Annales Geophysicae 10472009) 27. <https://doi.org/10.5194/angeo-27-1047-2009>
- [3] D. A. Imel, Evaluation of the TOPEX/POSEIDON dual-frequency ionosphere correction, J. Geophys. Res., 99 (1994) 24895–24906, <https://doi.org/10.1029/94JC01869>

- [4] B. Opperman, P. Cilliers, L. A. Mckinnell & R. Haggard, Development of a regional GPS-based ionospheric TEC model for South Africa, *Advances in Space Research* 39 (2007) 808-815, <https://doi.org/10.1016/j.asr.2007.02.026>
- [5] J. A. Klobuchar, Design and characteristics of the GPS ionospheric time delay algorithm for single frequency users. In *PLANS'86-Position Location and Navigation Symposium* (1986) pp. 280-286.
- [6] T. L. Beach, T. R. Pedersen, M. J. Starks, & S. Y. Su, Estimating the amplitude scintillation index from sparsely sampled phase screen data, *Radio Science* 39 (2004).
- [7] X. Pi, A. Mannucci, U. J. Lindqwister & C. M. Ho, Monitoring of Global Ionospheric Irregularities Using the Worldwide GPS Network. *Geophysical Research Letters - GEOPHYS RES LETT* 24 (1997) 2283-2286. <https://doi.org/10.1029/97GL02273>
- [8] M. Wang, F. Ding, W. Wan, B. Ning & B. Zhao, monitoring global traveling ionospheric disturbances using the worldwide GPS network during the October 2003 storms, *Earth Planets Space* 59 (2007) 407-419. <https://doi.org/10.1186/BF03352702>
- [9] N. Jakowski, B. Yannick, F. De, G. Franceschi, M. Pajares, K. Jacobsen, I. Stanislawska, L. Tomasik, R. Warnant & G. Wautelet, Gilles, Monitoring, tracking and forecasting ionospheric perturbations using GNSS techniques, *Journal of Space Weather and Space Climate* 2 (2012) A260000. <https://doi.org/10.1051/swsc/2012022>
- [10] X. Pi, A. J. Mannucci, B. Valant-Spaight, Y. Bar-Server, L. J. Romans, S. Skone, L. Sparks & G. M. Hall, Observations of global and regional ionospheric irregularities and scintillation using GNSS tracking networks. Paper presented at proceedings of ION 2013 Pacific PNT meeting, Honolulu, HI, USA, (2013) 752-761.
- [11] R. Sieradzki, I. V. Cherniak & A. Krankowski, Near-real time monitoring of the TEC fluctuations over the Northern Hemisphere using GNSS permanent networks, *Advances in Space Research* 52 (2013) 391-402. <https://doi.org/10.1016/j.asr.2013.03.036>
- [12] X. Liu, Y. Yuan, B. Tan & M. Li, Observational Analysis of Variation Characteristics of GPS-Based TEC Fluctuation over China, *ISPRS International Journal of Geo-Information* 5 (2016) 237. <https://doi.org/10.3390/ijgi5120237>
- [13] G. Li, , B. Ning, & H. Yuan, Analysis of ionospheric scintillation spectra and TEC in the Chinese low latitude region, *Earth Planets and Space* 59 (2007) 279-285. <https://doi.org/10.1186/BF03353105>
- [14] Z. Yang & Z. Liu, Correlation between ROTI and Ionospheric Scintillation Indices using Hong Kong low-latitude GPS data, *GPS Solutions* (2015) <https://doi.org/10.1007/s10291-015-0492-y>
- [15] S. Basu, K. Groves, J. M. Quinn & P. Doherty, A Comparison of TEC Fluctuation and Scintillations at Ascension Island, *Journal of Atmospheric and Solar-Terrestrial Physics* 61 (1999) 1219-1226. [https://doi.org/10.1016/S1364-6826\(99\)00052-8](https://doi.org/10.1016/S1364-6826(99)00052-8)
- [16] S. Thombre, S. Söderholm, H. Z. Bhuiyan, Mohammad, M. Kirkko-Jaakkola, L. Ruotsalainen & H. Kuusniemi, Investigating the Indian Regional Navigation Satellite System using a Software Multi-GNSS Receiver in Europe (2005) .
- [17] S. K. Upadhyaya, G. S. Pettygrove, J. W. Oliveira & B. R. Jahn, An introduction—global positioning system. calospace.ucdavis.edu/Docs/Intro-GPS-Final.pdf (2005)